Tissue Eng Regen Med (2018) 15(3):351–361
https://doi.org/10.1007/s13770-018-0115-0

Online ISSN 2212-5469
Print ISSN 1738-2696

ORIGINAL ARTICLE

Schwann Cells Enhance Penetration of Regenerated Axons into Three-Dimensional Microchannels

Chun Liu[1,3] · Jeremy Kray[1] · Christina Chan[1,2]

Received: 27 December 2017 / Revised: 12 January 2018 / Accepted: 28 January 2018 / Published online: 28 February 2018

Abstract Nerve regeneration after injury requires proper axon alignment to bridge the lesion site and myelination to achieve functional recovery. Transplanted scaffolds with aligned channels, have been shown to induce axon growth to some extent. However, the penetration of axons into the microchannels remain a challenge, influencing the functional recovery of regenerated nerves. We previously demonstrated that the size of microchannels exerts significant impact on Schwann cells (SCs) migration. Here we demonstrate that migration of SCs promotes, significantly, the dorsal root ganglion (DRG) neurons to extend axons into three-dimensional channels and form aligned fascicular-like axon tracts. Moreover, the migrating SCs attach and wrap around the aligned axons of DRG neurons in the microchannels and initiate myelination. The SCs release growth factors that provide chemotactic signals to the regenerating axons, similar to the response achieved with nerve growth factor (NGF), but with the additional capability of promoting myelination, thereby demonstrating the beneficial effects of including SCs over NGF alone in enhancing axon penetration and myelination in three-dimensional microchannels.

Keywords Nerve regeneration · Axon length · Schwann cell migration · Scaffold · Microchannel

1 Introduction

In both the central nervous system (CNS) and the peripheral nervous system (PNS) axons regenerates for a period, followed by demyelination, leading to failure of the axons to fully regenerate after nerve injury [1], resulting in permanent deficits of motor, sensory or autonomic function. Limited axonal plasticity occurs during nerve regeneration after injury because of the presence of inhibitory molecules both in the extracellular matrix [2] and myelin [3]. In addition, the lack of appropriate spatial and temporal gradients in the growth factor to promote growth of the axons [4, 5].

Tissue engineered scaffolds could aid the organized growth and guidance of axons across the injury site after spinal cord injury (SCI) jury [6–8]. Tremendous strides have been made to enhance the alignment, length, thickness, and myelination of the injured axons. For example, bone marrow stromal cells expressing neurotrophin-3 (NT-3) were seeded in templated agarose scaffolds, which induced 83% of the axons to grow over a 2 mm distance [9]. Concomitantly, we demonstrated that axons of dorsal root ganglion (DRG) neurons can successfully be induced to align, grow in thickness, and myelinate on a pre-stretched anisotropic surface [10], emphasizing the importance of anisotropy on tissue regeneration. Despite growing and

✉ Christina Chan
krischan@egr.msu.edu

[1] Department of Chemical Engineering and Materials Science, Michigan State University, 428 S. Shaw, 2100EB, Lane, East Lansing, MI 48824, USA

[2] Department of Biochemistry and Molecular Biology, Michigan State University, 428 S. Shaw Lane, 2100EB, East Lansing, MI 48824, USA

[3] Present Address: Center for Molecular Imaging, Department of Radiology, Medical School, University of Michigan, 109 Zina Pitcher Place, Ann Arbor, MI 48109, USA

Table 1 Materials and company list

Material	Company
Poly-L-lysine	Trevigen (Gaithersburg, MD)
Sodium bicarbonate	Sigma-Aldrich (St. Louis)
Poly-D-lysine	Sigma-Aldrich (St. Louis)
Fluoro-2 deoxy-uridine	Sigma-Aldrich (St. Louis)
Uridine	Sigma-Aldrich (St. Louis)
Cytosine β-D-arabinofuranoside (AraC)	Sigma-Aldrich (St. Louis)
Anti-Thy 1.1 antibody (cat. no. M-7898)	Sigma-Aldrich (St. Louis)
Rabbit complement	Sigma-Aldrich (St. Louis).
Heat inactivated fetal bovine serum	Hyclone (Logan, Utah)
Bovine pituitary extract (BPE)	Clonetics (Allendale, NJ)
Forskolin	Calbiochem (Billerica, MA)
Type I collagenase	Worthington (Lakewood, NJ)
Neurobasal medium 1×	Invitrogen (Carlsbad, CA)
B-27 supplement	Invitrogen (Carlsbad, CA)
Glutamax-I	Invitrogen (Carlsbad, CA)
Albumax-I	Invitrogen (Carlsbad, CA)
Nerve growth factor	Invitrogen (Carlsbad, CA)
Dulbecco's modified Eagle medium (DMEM)	Invitrogen (Carlsbad, CA)
Penicillin and streptomycin	Invitrogen (Carlsbad, CA)
0.25% trypsin–EDTA	Invitrogen (Carlsbad, CA)
1× phosphate buffered saline (PBS)	Invitrogen (Carlsbad, CA)
HEPES buffer	Invitrogen (Carlsbad, CA)
Fluo-4 AM	ThermoFisher Scientific (Grand Island, NY)
Cell permeant (cat. no. F-14201)	ThermoFisher Scientific (Grand Island, NY)
Bovine serum albumin (BSA)	US Biological (Marblehead, MA)
Rabbit anti-myelin protein zero antibody (cat. no. ab31851)	Abcam (Cambridge, MA)
Mylar films	InfinityGraphics (East Lansing, MI)
Type I collagen (cat. no. #354236)	Corning (Corning, NY)

promising results of animal models, challenges remain in achieving functional recovery for nerve injury repair that traverses long distance. Multiple factors contribute to this failure, including disruption of the axon growth, molecules secreted by the scar tissue that inhibit axon growth, lack of molecules that promote axon growth, and partial remyelination [11–13]. Therefore, a multifaceted strategy is required to address these challenges, namely the engineered scaffold needs to be able to deliver growth factors and promote myelination, in addition to enhancing axon growth and alignment.

Schwann cells (SCs) are critical to the survival and function of neurons in the PNS. They maintain and aid axon regeneration [14], and promote axon growth by providing trophic support [15]. SCs secrete glial cell line-derived neurotrophic factor (GDNF) and NT-3, which participate substantially in promoting axon growth [16, 17]. Transplanting engineered SCs to secrete growth factors enhanced axonal regeneration, and improved function [18]. SCs also migrate into the CNS and remyelinate axons SCI [19, 20]. Since SCs secrete multiple growth factors, their inclusion show promise in therapeutic strategies for spinal cord repair [21–24]. In light of these benefits of SCs [25–27], we propose that SCs coupled with 3D channel scaffolds could aid axon regeneration in SCI. Previously we demonstrated that the scaffold channels size strongly influenced the speed migration of SCs [20]. In this study, we extend our design of multifunctional scaffold to incorporate both neurons and SCs within linear channels, and characterized their synergistic effects on axon growth as a function of channel size.

We hypothesize that the axon growth in channels are influenced by both the channel size and SC migration, as migrating SCs not only offer trophic support to the regenerating axons but also provide myelination. We designed micropatterned channels using polydimethylsiloxane (PDMS) and co-cultured DRG neurons with SCs for 21 days to investigate the presence of migrating SC on the penetration of axon into the channels. The results demonstrate that the migrating SCs through the

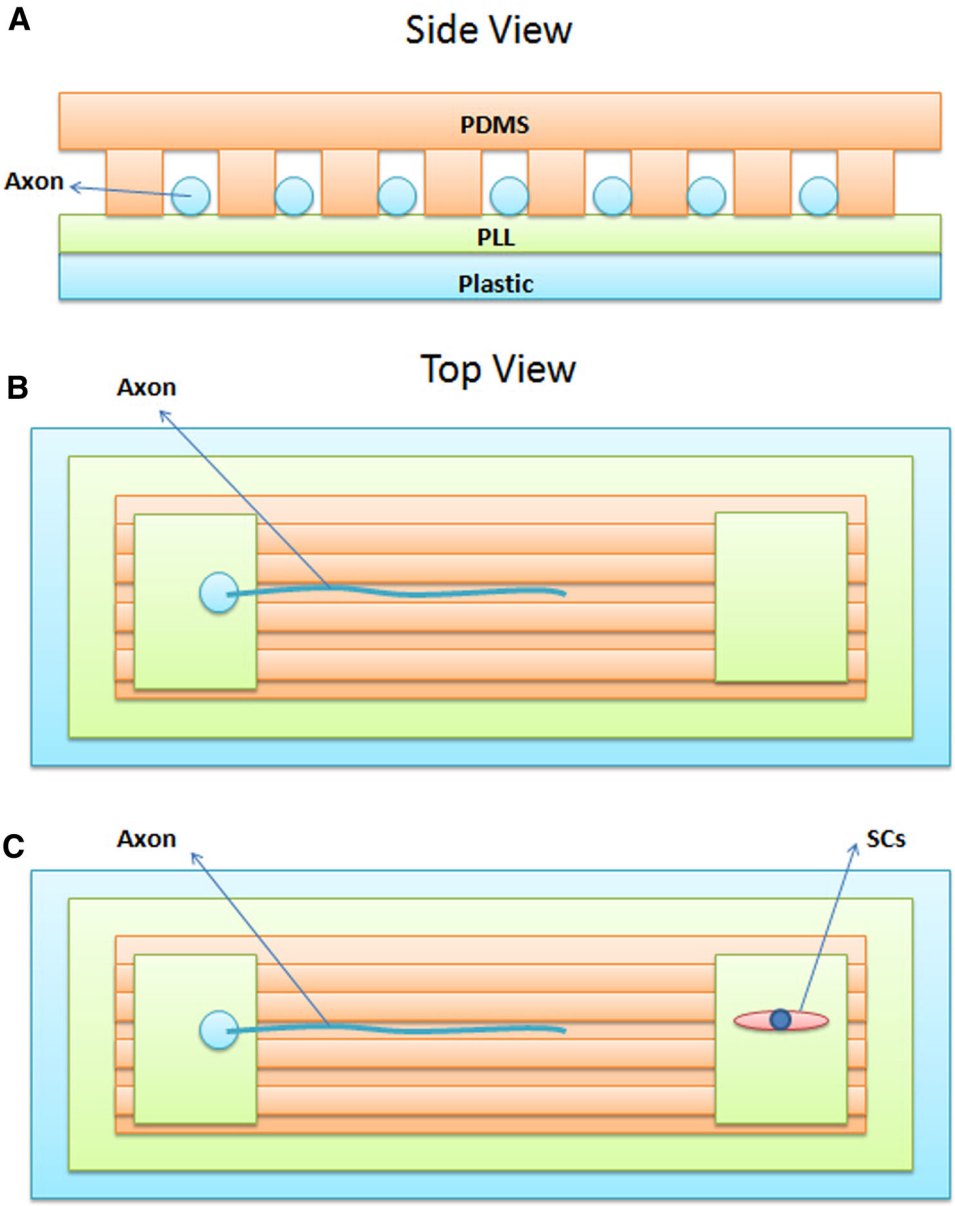

Fig. 1 Design of micropatterned co-culture platform. **A** Side view of the sealed channels. A thin layer of PLL is coated onto polystyrene substrate before the micropatterned PDMS is attached to the substrate. The PDMS channel is placed side faced down to achieve sealed channels for the axons to grow and extend. **B** Top view of the platform. Freshly isolated DRG neurons are seeded onto one of the open area at one end of the channels, and the regenerating axons extend into the channels. The open area on the opposite side remains empty as the negative control. **C** To promote axon extension, SCs are seeded on the open area (opposite to the DRGs) as the regenerating DRG axons approach that end of the channels

microchannels contributed to increasing the penetration depth of the axons. In addition, the migrating SCs attached to the penetrating axons and produced components of the myelin sheath. The SCs were found to induce similar positive effects as the release of nerve growth factor (NGF) from a collagen gel on the axon penetration but with the added benefit of myelination. We show that using microchannels, the linear axonal regeneration is enhanced, as is the migration of the SC.

2 Materials and methods

2.1 Materials

PDMS substrates were prepared as described previously in [10, 20]. Table 1 provides a materials list.

2.2 Patterned microchannel cell co-culture system fabrication

The design of the patterned microchannel cell culture system is shown in Fig. 1. Micropatterned PDMS channels are prepared as previously described [20]. Two cut squares are placed at the two ends of the channels for seeding the cells. The channel pattern is placed upside down (faced

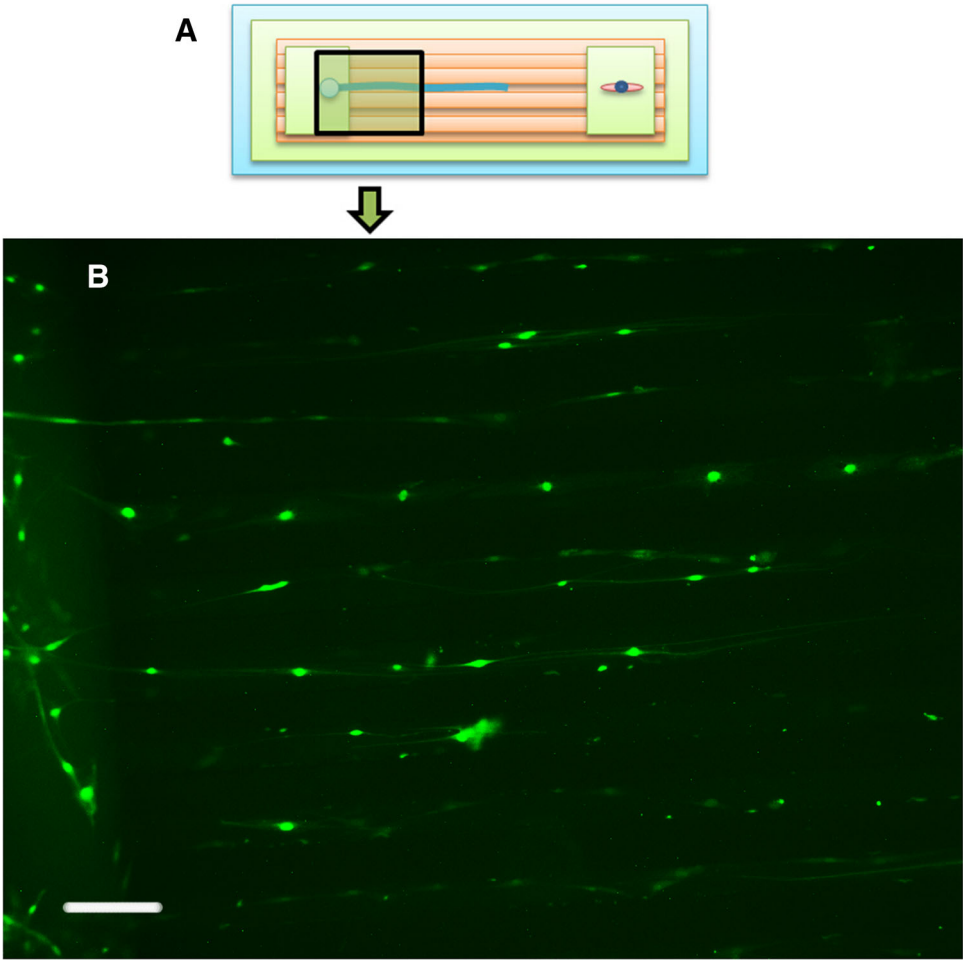

Fig. 2 Regenerating axons in 50 μm channels with addition of the SCs. **A** Freshly isolated DRG neurons are seeded and cultured for 5–6 days in the open area to allow the axons to grow and extend through the channels, whereupon SCs are subsequently seeded on the open area at the opposite end of the channels. **B** After 21 days of culture, Fluo-4 is added to permit fluorescent images of live cell staining with ×10 objective. Scale bar indicates 100 μm

down) and attached tightly to the PLL coated polystyrene substrate to seal the channels to the substrate. To prevent the cells from being flushed out of the channels, we used crosslinked collagen gel (375 μl type I collagen + 27 μl NaHCO3 + 50 μl DMEM) as a glue to seal the edges.

2.3 DRG neuron and schwann cell isolation and culture

The cell isolation procedures were approved by the Institutional Animal Care and Use Committee at Michigan State University (IACUC no. 10/13-227-00). All applicable international, national, and/or institutional guidelines for the care and isolation of cells from the animals were followed.

5–8 day-old Sprague–Dawley rats were used to isolate DRG neurons as described in our previous published protocol [28]. In brief, we sacrifice rats by decapitation, and cut away the skin that overly as well as any excess tissue on the spinal cord. We completely remove the spine from the body and extract the spinal cord. We use a fine pair of tweezers and a pair of microsurgery scissors, to collect approximately 10–16 DRGs from both sides. We trim the nerve roots and transfer the DRGs to 5 ml of ice-cold Hanks' Balanced Salt Solution (HBSS) buffer that contains 1 ml penicillin/streptomycin. We transfer the dissection medium with the DRGs to a new 15-ml tube, and centrifuged at 900 RCF at 4 °C for 5 min. We remove the supernatant after centrifugation, and incubate the DRGs in 6 ml of 0.05% Trypsin–EDTA (1×) (Sigma; 1 mg/ml, 45 min) at 37 °C and followed by incubation in 2 ml collagenase (Sigma; 500 U/ml, 20 min) at 37 °C. We centrifuge the ganglia at 900 RCF in 4 °C for 5 min after chemical dissociation and then remove the supernatant. We further resuspended the pellet in 10 ml of standard growth media and centrifuged, as described above. Next, we resuspended the cells in standard growth media containing Neurobasal medium, which contains 2% B27, 0.5% antibiotic (penicillin/streptomycin), 1% Glutamax, and 0.2% Albumax. We then plate the dissociated neurons on PLL coated pre-stretched surface and incubated at 37 °C at 5% CO_2.

We isolate SCs using the protocol as described previously [29] by decapitating one day old rats. We extract the

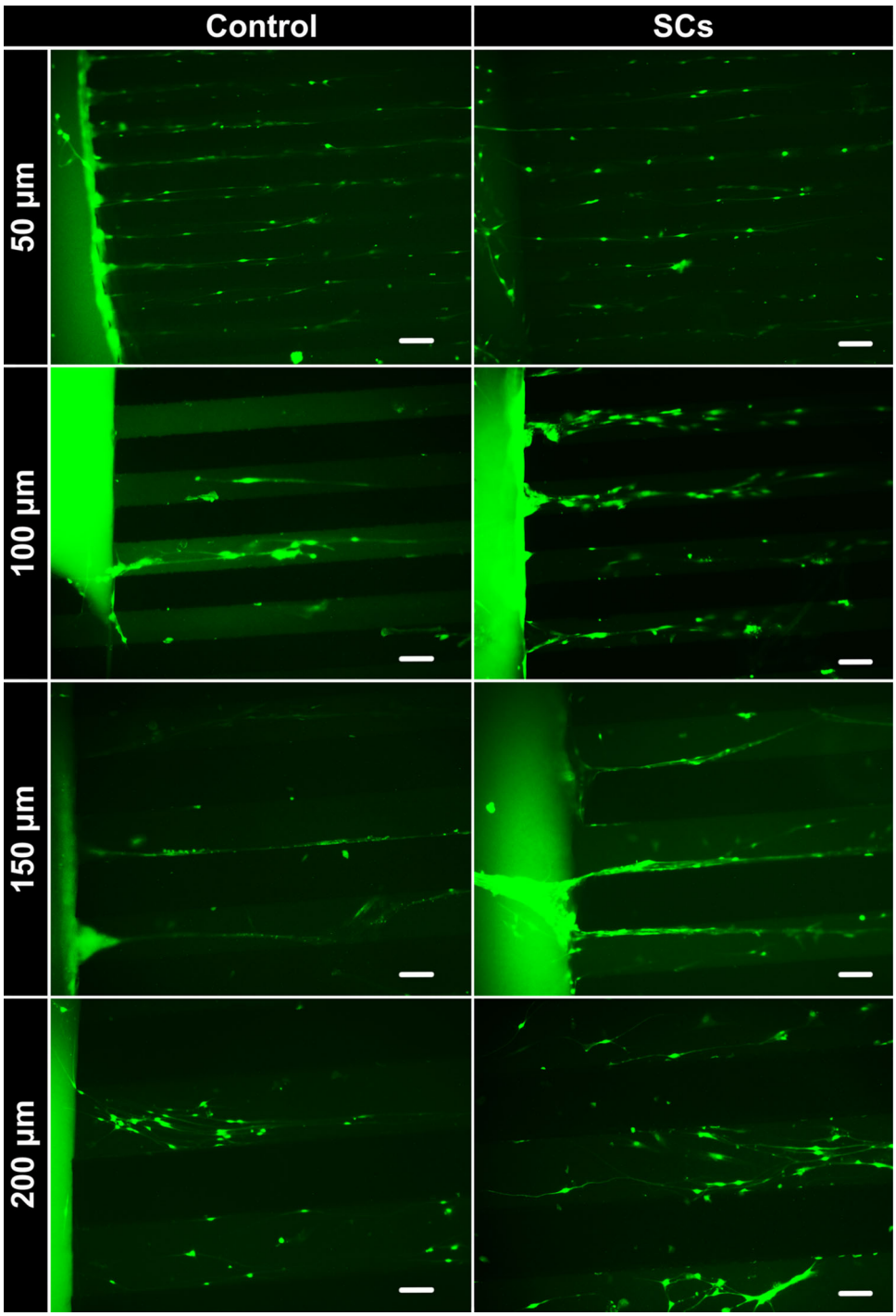

Fig. 3 Comparison of regenerated axons extending into channels with and without addition of the SCs. After 21 days of culture, fluorescent images are taken with ×10 objective. Scale bar indicates 100 µm

sciatic nerves by making an incision from the tail up the spine to the inner thigh near the foot. We cut the nerve sections into small pieces and transferred the sections to a dissociation medium that contains collagenase and trypsin (1:9 volume ratio) and incubate the sections for 45 min at 37 °C. We perform mechanical dissociation using fire polished glass pasteur pipette. We next centrifuge the cells for 5 min and resuspended the cells in DMEM containing 10% heat inactivated FBS and 1% antibiotic (penicillin/streptomycin). We add 4 mM AraC begins to the medium after 48 h of culture to begin the purification step, which is followed by antibody selection using 250 µl Anti-thy 1.1 antibody and 250 µl Rabbit Complement on day 5. We culture the cells in complete SC growth medium containing DMEM, 10% FBS, 1× Penn/Strep, 21 µg/ml BPE, and 4 µM forskolin, after the purification step, and placed the

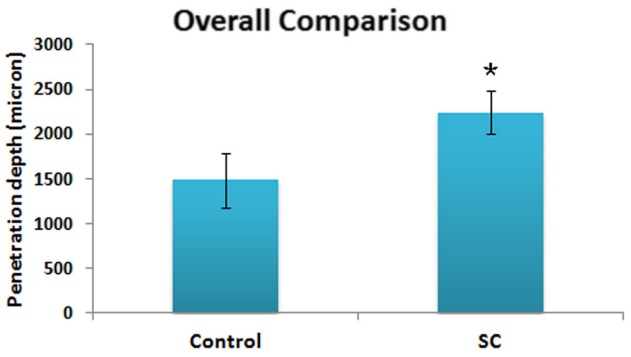

Fig. 4 Comparison of depth of axon extension into the channels with and without addition of the SCs. Axon extension is quantified after 21 days of culture for both the control and SC groups. The penetration depth ratio is defined as the penetration depth of the SC group divided by the control group. The average is across all 4 channel sizes (50, 100, 150 and 200 μm), and the standard errors are calculated from 5 replicates. *p value < 0.05

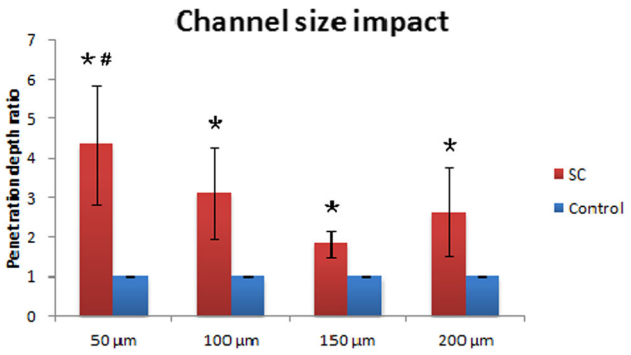

Fig. 5 The impact of channel size on axon extension in the presence of SCs. All the data are normalized to the control group for each biological replicate. *> control; #> 150 μm, p value < 0.05

cells in a humidified incubator containing 5% CO_2 at 37 °C. We replace the medium every 2 days until the cells reach 80–90% confluence. We detach the confluent cells using 0.25% trypsin–EDTA and re-plated the cells at a density of 5000 cells per mL, adding 100 μl of cells to one of the open squares.

We seed freshly isolated DRG neurons in one of the open area, and cultured the DRGs for 5–6 days to allow the axons to grow and extend through the channels, whereupon SCs are subsequently seeded on the open area at the opposite end of the channels.

2.4 Fluorescent imaging

We visualize the penetration of axons into the channels using fluorescent live cell imaging. We add 1 μl of Fluo-4 into each well and incubate the cells at 37 °C for 30 min. We obtain fluorescent images using a 10× objective Leica DM IL inverted microscope (Bannockburn, IL) that is equipped with SPOT RT color camera (Diagnostics Instruments, MI).

2.5 Collagen gel pre-loaded with NGF

We prepare the collagen gel by adding 10% reconstruction buffer (4.77 g HEPES, 2.2 g $NaHCO_3$ and 0.2 g NaOH in 100 ml H_2O) and DMEM to a type I collagen solution at a final concentration of 2 mg/mL collagen. To crosslink the collagen gel, we incubate the mixed gel overnight at 37 °C. We reconstitute the NGF to 100 mg/ml in sterile phosphate buffered saline (PBS, Sigma). We add 20 μl of NGF stock solution (50 μg/ml) to 1 ml collagen gel before crosslinking to pre-load NGF into the collagen gel.

2.6 Axon penetration depth quantification

We define the axon penetration depth as the furthest position the axons reach under each condition for each channel size. We quantify the axon penetration depth, by placing a stage micrometer on the objective to measure the diameter through the field viewed using the eye pieces. We use the microscope to quantify the axon penetration depth by measuring the length of successive live images starting from the end of channels with DRGs to the furthest end of the axons. The penetration depth ratio is defined as penetration depth of the SC group divided by the control group. We quantified 5 biological replicates. Each batch contained at least 4 replicates of each condition and channel size.

2.7 Statistical analyses

We express all the data as mean ± standard deviation. We used the ANOVA-Tukey's test in Fig. 5 to assess for significance. We used a two-sample Student's t test in Fig. 8C to determine statistical significance. In all cases, statistical significant is determined by p values of < 0.05.

3 Results and discussion

3.1 Design of patterned channel cell co-culture system

DRGs and SCs are co-cultured at opposite ends of the micropatterned channels of different size channels (50, 100, 150, and 200 μm) as shown in Fig. 1. The patterned side of PDMS is attached to the PLL coated plastic surface, forming sealed channels, allowing unidirectional axon penetration (Fig. 1A). Freshly isolated DRGs are seeded at one end of the channels such that the cells are attached to the open area. The other end of the channels, is either left blank (Fig. 1B) as a negative control, or seeded with SCs

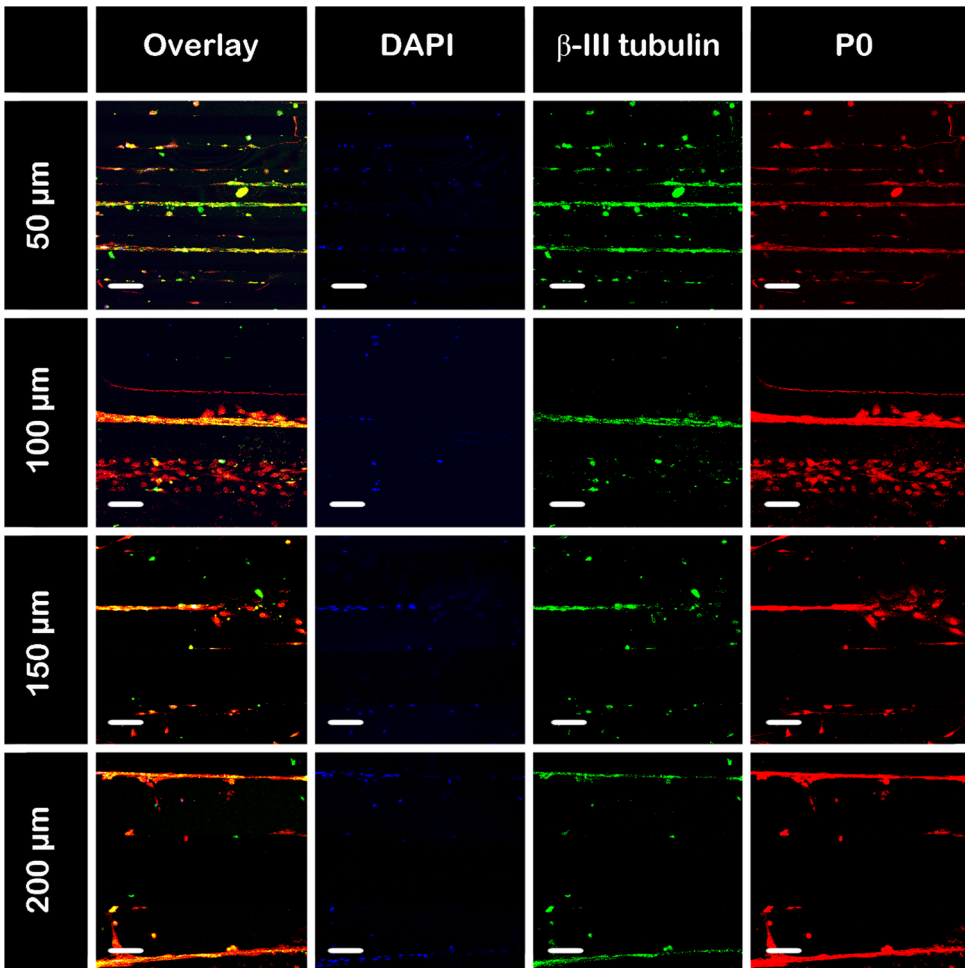

Fig. 6 Co-localization of SCs with regenerating axons. After 21 days of culture, the co-cultures of DRG neurons with SCs in the different size channels are stained with anti-mouse β-III tubulin (green) to indicate axons, P0 (red) to indicate SCs, and DAPI (blue) to indicate nuclei. First column represents an overlay of all three markers. Fluorescent images are taken with ×20 objective. Scale bar indicates 100 μm. (Color figure online)

(Fig. 1C). As the axons grow and penetrate towards the start (other end) of the channels, SCs are seeded at the other end of the channels and begin to migrate towards the axons and to provide growth factors.

3.2 Axons penetration into patterned channels

Figure 2 shows the regenerating axons penetrating into the 50 μm channels towards the SCs after 21 days of culture. The bottom fluorescent image shows the axons penetrating from the open area into the channel, with the axon fibers traversing along the vertical edge at the start of channels (on the left side of the image). The axons penetrate into the channels and align in the channel direction. The bright dots in the channels indicate cell body of the migrating DRG neurons. The overall penetration depth of the axons into the channels is the result of the aligned axon length (in the channel direction) and the migration distance of the DRG cell bodies. We cannot decouple the growth of the axon length from the cell body migration, as this would occur during *in vivo* transplantation, whereby nerve regeneration involves both increasing the length of the axons and migrating neurons. From this fluorescent image, we also found migrated SCs both located in the channels and overlaid with axons, which will be further illustrated by immunostaining in Sect. 3.4.

Figure 3 shows the comparison of the axons penetrating into different sized channels with and without the SCs addition. In the smaller channels (50 and 100 μm), single axons aligned straight and penetrated the channels, while in the larger channels (150 and 200 μm), multiple axons penetrated and with some degree of curvature. In the 150 and 200 μm channels, the axons appear to cluster together to form fascicular-like bundles. Additionally, in the 200 μm channels, more axons are found to penetrate and appear to form a network.

3.3 Comparison of axon penetration depth under different conditions

Figure 4 shows the axons successfully penetrate into the channels both with and without SCs addition. To quantitatively demonstrate the impact of SCs addition on the axon penetration, we measured the axon penetration depth

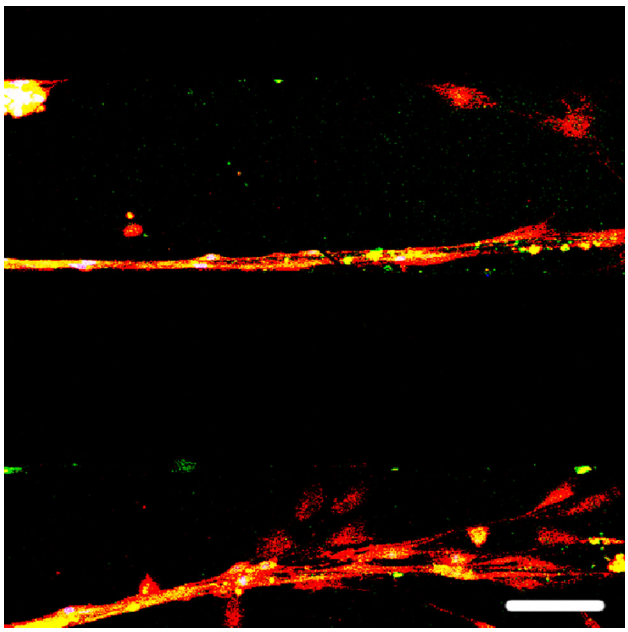

Fig. 7 SCs aligned with regenerated axons. An overlay image of a co-culture of DRG neurons with SCs in a 200 μm channel shows the SCs align with the axons to form neat thick bundles, but are dispersed at the end of the axons. Cells are stained with anti-mouse β-III tubulin (green) to indicate axons, P0 (red) to indicate SCs, and DAPI (blue) to indicate nuclei. Fluorescent images are taken with ×20 objective after 21 days of culture. Scale bar indicates 100 μm. (Color figure online)

after 21 days of culture. Figure 5 shows the average penetration depth of the DRG axons with and without SCs addition in the 4 different sized channels. The addition of SCs increase significantly the penetration depth of the DRG axons into the channels. Therefore, the SCs at the other side of the channels stimulate the neurons to penetrate further into the channels. To further investigate the impact of the channel size on the penetration of the axons, the distance traversed in each channel size are normalized to the control group of the same sized channels (Fig. 5). For the 50, 100, and 150 μm channels, the extension of the axons increased as the channel size decreased, with the 50 μm channels significantly promoting axon extension as compared to the larger 150 μm channels. This trend is similar to what was observed in our previous SC migration study, where the SC migration speed on the micropatterned channels (50, 100, and 150 μm) increased as the channel size decreased [20]. Therefore, the greater penetration depth of the DRG axons correlates with the fastest migration speed of the SCs in the smallest channels. It is unclear why there is a slight increase in the axon extension in the 200 μm channels over the 150 μm channels. This might be due to the wider space allowing more cells to migrate into the channel. These results indicate that the channel size exerts an effect on the axon extension.

3.4 Co-localization of SCs with regenerated axons

Figures 2 and 3 show live staining of both SCs and DRGs migrating through the channels. To clearly indicate the location of the migrating SCs and the relationship between the SCs and axons, we perform immunostaining on both the DRG neurons and SCs after 21 days of culture in the channels. Additionally the SCs migrate in the channels and attach onto the axons, as illustrated by immunostaining in Fig. 6. As shown in Fig. 6, the axons are stained for β-III tubulin (green), the SCs are stained for P0 (red), a marker of mature SCs and a myelin sheath component, and the cell nuclei are stained with DAPI (blue). In the 50 μm channels, SCs attached to the axons, while in the wider channels, in addition to myelinating the axons, more SCs have migrated into the channels as indicated by the P0 staining in the overlay images. In all the channels, SCs are found attached to the axons and expressing the myelin component P0. Therefore, the addition of SCs to this channel system not only enhances axon penetration, but also initiates the myelination process on the regenerated axons, which is significant for functional nerve recovery.

Figure 7 shows the myelination of fascicle-like axon bundles in the 200 μm channels. In the top channel, several axons are bound together and form a fascicle-like bundle, with the SCs attaching along the axons. In the bottom channel the SCs are dispersed at the end of the axons, showing a scattered “tail”. This image shows two different patterns of SCs in the channels, either attached or wrapped around the axons and thus forming a co-localize pattern involving myelination; or dispersed attachment on the substrate with a flat cell morphology, similar to what is observed in cultures of SCs. Nonetheless, the images support that the migration of SCs in the patterned channels facilitates myelination of the regenerated axons.

3.5 Penetration of the regenerated axons into channels with NGF release

The addition of SCs offer two main advantages. First SCs are known to secret growth factors that are beneficial to axon growth, and second the migrating SCs decrease the distance for the secreted growth factors to diffuse before reaching the axons. To further examine the effects of SCs addition, we designed a positive control using NGF in the same channel system. The design of the positive control consists of a collagen gel pre-loaded with NGF that is added to the other side of the channels in lieu of the SCs (Fig. 8A). A previous study demonstrated a sustained release of NGF from crosslinked collagen gel enhances cell growth [30]. Here, the NGF-embedded collagen gel provides sustained NGF release which diffuses into the channels to induce chemotaxis and attract axons to extend

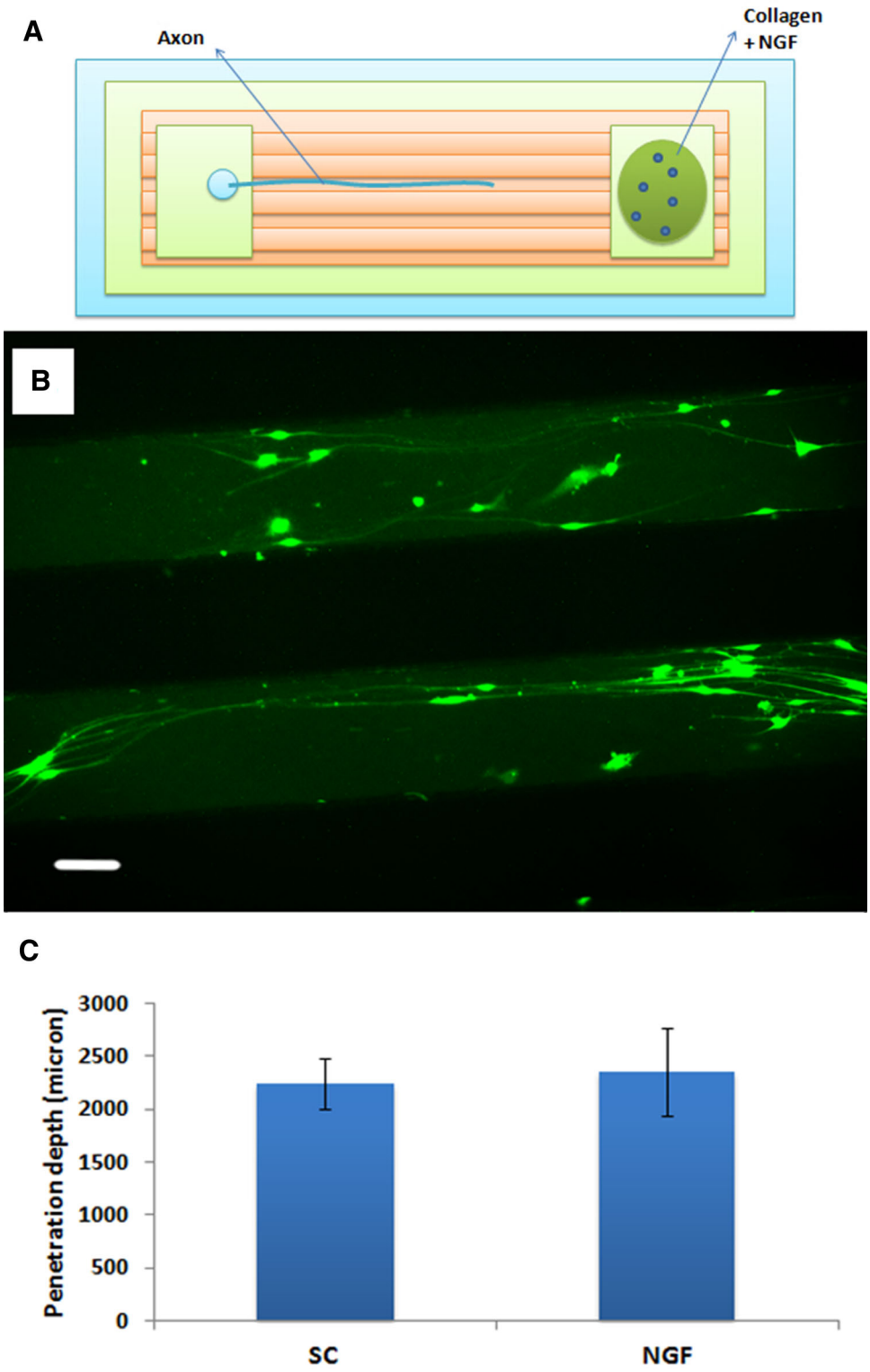

Fig. 8 Regenerating axons extend into channels with NGF release. **A** Collagen gel pre-loaded with NGF is added to the other end of the channels. **B** Axons extend into a 200 μm channel with NGF being released from the other end of the channels. **C** Comparison of axon extension into channels between the SCs and the NGF groups

from the opposite side. The axons extend into the 200 μm channels to form axon bundles, similar to the SC group (Fig. 8B). The average penetration depth of the axons with NGF release are quantified against the SC group (Fig. 8C). There is no significant difference between the SC and NGF groups for all the channels, indicating the SCs exert a similar effect on the axon extension to the NGF released from the collagen gel. These results lend support to our hypothesis that the addition of SCs in this channel system offers trophic support to the regenerating axons to promote

axon extension. Future studies could quantify the growth factors released from the SCs, by developing a computational model of the growth factor gradient secreted by the migrating SCs in the channels.

In summary, we developed a patterned microchannel system for evaluating the penetration of regenerating axons with the aid of SC migration. The SCs enhance axon penetration while the channel size exerts an effect on both the SC migration and axon extension. The SCs offer trophic support to the regenerating axons, with similar effects to the NGF. The SCs migrate and attach to the axons and initiate myelination. The results from this study could inform on future design of transplantable scaffolds for nerve tissue regeneration.

Acknowledgements We thank Dr. Melinda Frame from the Center for Advanced Microscopy at Michigan State University for help with confocal microscopy imaging. We thank Xiaopeng Bi for their assistance with the photolithography process at Michigan State University. Funding was provided by Division of Chemical, Bioengineering, Environmental, and Transport Systems (Grant Nos. CBET 1510895 and CBET 1547518) and National Cancer Institute (Grant No. R21CA176854).

Compliance with ethical standards

Conflict of interest The authors do not have a conflict of interest to declare. This manuscript has not be submitted elsewhere.

Ethical statement All applicable international, national, and/or institutional guidelines for the care and use of animals were followed. The cell isolation procedures were approved by the Institutional Animal Care and Use Committee at Michigan State University (IACUC no. 10/13-227-00). This article does not contain any studies with human participants performed by any of the authors.

References

1. Totoiu MO, Keirstead HS. Spinal cord injury is accompanied by chronic progressive demyelination. J Comp Neurol. 2005;486:373–83.
2. Silver J, Miller JH. Regeneration beyond the glial scar. Nat Rev Neurosci. 2004;5:146–56.
3. Schwab ME. Nogo and axon regeneration. Curr Opin Neurobiol. 2004;14:118–24.
4. Blesch A, Tuszynski MH. Spinal cord injury: plasticity, regeneration and the challenge of translational drug development. Trends Neurosci. 2009;32:41–7.
5. Liu C, Pyne R, Baek S, Sakamoto J, Tuszynski MH, Chan C. Axonal regeneration and myelination: applicability of the layer-by-layer technology. Layer-by-layer films for biomedical Applications. Weinheim: Wiley-VCH Verlag GmbH & Co. KGaA; 2015. p. 525–46.
6. Hurtado A, Moon LD, Maquet V, Blits B, Jérôme R, Oudega M. Poly (D,L-lactic acid) macroporous guidance scaffolds seeded with Schwann cells genetically modified to secrete a bi-functional neurotrophin implanted in the completely transected adult rat thoracic spinal cord. Biomaterials. 2006;27:430–42.
7. Moore MJ, Friedman JA, Lewellyn EB, Mantila SM, Krych AJ, Ameenuddin S, et al. Multiple-channel scaffolds to promote spinal cord axon regeneration. Biomaterials. 2006;27:419–29.
8. Stokols S, Tuszynski MH. The fabrication and characterization of linearly oriented nerve guidance scaffolds for spinal cord injury. Biomaterials. 2004;25:5839–46.
9. Gros T, Sakamoto JS, Blesch A, Havton LA, Tuszynski MH. Regeneration of long-tract axons through sites of spinal cord injury using templated agarose scaffolds. Biomaterials. 2010;31:6719–29.
10. Liu C, Pyne R, Kim J, Wright NT, Baek S, Chan C. The impact of prestretch induced surface anisotropy on axon regeneration. Tissue Eng Part C Methods. 2016;22:102–12.
11. Chen BK, Knight AM, de Ruiter GC, Spinner RJ, Yaszemski MJ, Currier BL, et al. Axon regeneration through scaffold into distal spinal cord after transection. J Neurotrauma. 2009;26:1759–71.
12. Pawar K, Cummings BJ, Thomas A, Shea LD, Levine A, Pfaff S, et al. Biomaterial bridges enable regeneration and re-entry of corticospinal tract axons into the caudal spinal cord after SCI: association with recovery of forelimb function. Biomaterials. 2015;65:1–12.
13. Tabesh H, Amoabediny G, Nik NS, Heydari M, Yosefifard M, Siadat SO, et al. The role of biodegradable engineered scaffolds seeded with Schwann cells for spinal cord regeneration. Neurochem Int. 2009;54:73–83.
14. Bhatheja K, Field J. Schwann cells: origins and role in axonal maintenance and regeneration. Int J Biochem Cell Biol. 2006;38:1995–9.
15. Riethmacher D, Sonnenberg-Riethmacher E, Brinkmann V, Yamaai T, Lewin GR, Birchmeier C. Severe neuropathies in mice with targeted mutations in the ErbB3 receptor. Nature. 1997;389:725–30.
16. Jessen KR, Mirsky R. The origin and development of glial cells in peripheral nerves. Nat Rev Neurosci. 2005;6:671–82.
17. Gordon T. Nerve regeneration: understanding biology and its influence on return of function after nerve transfers. Hand Clin. 2016;32:103–17.
18. Kanno H, Pressman Y, Moody A, Berg R, Muir EM, Rogers JH, et al. Combination of engineered schwann cell grafts to secrete neurotrophin and chondroitinase promotes axonal regeneration and locomotion after spinal cord injury. J Neurosci. 2014;34:1838–55.
19. Ghosh M, Tuesta LM, Puentes R, Patel S, Melendez K, El Maarouf A, et al. Extensive cell migration, axon regeneration, and improved function with polysialic acid-modified Schwann cells after spinal cord injury. Glia. 2012;60:979–92.
20. Liu C, Kray J, Toomajian V, Chan C. Schwann cells migration on patterned polydimethylsiloxane microgrooved surface. Tissue Eng Part C Methods. 2016;22:644–51.
21. Xu XM, Zhang SX, Li H, Aebischer P, Bunge MB. Regrowth of axons into the distal spinal cord through a Schwann-cell-seeded mini-channel implanted into hemisected adult rat spinal cord. Eur J Neurosci. 1999;11:1723–40.
22. Tetzlaff W, Okon EB, Karimi-Abdolrezaee S, Hill CE, Sparling JS, Plemel JR, et al. A systematic review of cellular transplantation therapies for spinal cord injury. J Neurotrauma. 2011;28:1611–82.
23. Xia H, Sun X, Liu D, Zhou Y, Zhong D. Oriented growth of rat Schwann cells on aligned electrospun poly(methyl methacrylate) nanofibers. J Neurol Sci. 2016;369:88–95.
24. Wang Y, Li WY, Jia H, Zhai FG, Qu WR, Cheng YX, et al. KLF7-transfected Schwann cell graft transplantation promotes sciatic nerve regeneration. Neuroscience. 2017;340:319–32.
25. Son YJ, Thompson WJ. Schwann cell processes guide regeneration of peripheral axons. Neuron. 1995;14:125–32.

26. Höke A, Redett R, Hameed H, Jari R, Zhou C, Li ZB, et al. Schwann cells express motor and sensory phenotypes that regulate axon regeneration. J Neurosci. 2006;26:9646–55.
27. Guest JD, Rao A, Olson L, Bunge MB, Bunge RP. The ability of human schwann cell grafts to promote regeneration in the transected nude rat spinal cord. Exp Neurol. 1997;148:502–22.
28. Liu C, Chan C. An approach to enhance alignment and myelination of dorsal root ganglion neurons. J Vis Exp. 2016. https://doi.org/10.3791/54085.
29. Mantuano E, Jo M, Gonias SL, Campana WM. Low density lipoprotein receptor-related protein (LRP1) regulates Rac1 and RhoA reciprocally to control Schwann cell adhesion and migration. J Biol Chem. 2010;285:14259–66.
30. Bhang SH, Lee TJ, Lim JM, Lim JS, Han AM, Choi CY, et al. The effect of the controlled release of nerve growth factor from collagen gel on the efficiency of neural cell culture. Biomaterials. 2009;30:126–32.